International Journal of Recent Technology and Engineering (IJRTE)
ISSN: 2277-3878 (Online), Volume-8 Issue-4, November 2019

Integration of Response Surface and Decision Support to optimize a Well Sidetrack under Uncertainty
II. Secondary Recovery Mechanism

Abisoye M. Mumuni, Oyinkepreye O. Orodu, Sunday S. Ikiensikimama

Abstract: ***The optimal time to sidetrack into a different layer from an already producing horizon with secondary recovery mechanism of waterflooding is evaluated with the uncertainties embedded in Probabilities of success (POS) including economic, operational, technical and reservoir properties. Previous literatures are majorly primary recovery and secondary recovery by waterflooding in which production profiles were represented by empirical and analytical models. However, not all recovery mechanisms can be sufficiently reproduced by these models and this introduces and explains the need for the use of proxy models to predict cumulative production and net-present-value (NPV).***

The peculiarity of this study is the application of decision analysis/tree with multiple terminal branches to both production and injection sidetrack, where NPV is estimated under the influence of change of recovery mechanism due to sidetrack (recompletion) to another possibly non-communicating zone or layer with uncertainty of reservoir properties and production discontinuity from the already producing horizon.

By and large, sidetrack time adds in acute non-linearity on the NPV. Multi–objective functions of proxy models over time-intervals for the impacted terminal branches, known as split design was applied to evaluate when to carry out a well sidetrack operation under risk and uncertainty. This was adopted to resolve severe non-linearity of the NPV and the multi-objective function of EMV by a standard optimization algorithm in a spreadsheet. The final results gave a satisfactory match to the simulation results. In order to get a perfect match through more improvements on performance there is a need for large computation times and the decision must be made depending on the required result. Monte- Carlo simulation analysis shows that optimal sidetrack time is at the early production life.

Keywords: Sidetrack, multi-objective optimization, Experimental Design, decision analysis, net-present-value

I. INTRODUCTION

This is the second paper in the series of optimizing well sidetrack using design of experiments and decision tree analysis while the first paper considers primary recovery, this paper considers using waterflooding as a secondary recovery mechanism. Analytical models according to Orodu et al., (2011) did not replicate the flow adequately which promotes the need for the application of proxy model. Uncertainty is analyzed using experimental design (ED or DOE), response surface, Monte Carlo simulation, decision tree. These are all statistical methods (Dejean & Blanc, 1999).ED considers uncertainties and reduces the time used for runs to get response variables (Jourdan & Zabalza-Mezghani, 2004; Prada & Cunha, 2008; Murtha et al., 2009). For further details on the workings of Experimental Design (Dejean & Blanc, 1999; Prada & Cunha ,2008) are quite explanatory.

There is an issue of non-linearity or curvature as stated in the first paper in the series. The relationship between the response and factor is non-linear. This is obvious from the works of Li et al. (2011), Yeten et al. (2005), Dejean & Blanc (1999) and de Amorim & Moczydlower (2007). To solve non-linearity there can be increase in the level of each factor in the experimental design that are relevant to the response. This non-linearity can be caused by the introduction of a secondary recovery mechanism or just production discontinuity from the already producing horizon in primary recovery. Lawal (2009), suggested that the non-linearity can be solved by proxy models chosen for designated time intervals to match the prevailing physical flow mechanism underplay. There is the study of the risk in sidetrack operations as found in probability of success (POS) which was examined for primary and secondary recovery mechanism by Lerche & Mudford (2001) and Orodu et al. (2011) respectively. The objective was to calculate sidetrack time under production predictions centred on analytical equations and risk based on NPV. However, the equations for the secondary recovery were modelled around simulation results of a synthetic reservoir. The objective function, EMV which is a product of NPV and probability is optimized, the maximum EMV gives the optimized time. This is a decision analysis issue (Fig. 1) on the bases of ongoing production (and injection) from Zone-B (Fig. 2) and later sidetracking (recompletion) into Zone-A at a particular optimal time. POS of the sidetrack originates from the perceived success of continuous production (P_B) and injection (P'_B) for Zone-B, the zone initially under exploitation and that of successful sidetrack (P_A and P'_A) leading to production from Zone-A and injection into Zone-A.

Manuscript published on November 30, 2019.
* Correspondence Author
Abisoye M. Mumuni, (Dalhousie University) & PhD Student, CEFOR-ACE, World-Bank University of Port-Harcourt, Nigeria.
Oyinkepreye O. Orodu, Professor, Head of Department, Petroleum Engineering, Covenant University, Nigeria.
Sunday S. Ikiensikimama , Associate Professor, Department of Petroleum & Gas Engineering, University of Port Harcourt, Nigeria.

The NPV of each branch of the decision tree shall be evaluated in this study by proxy models with uncertainties of reservoir rock property of Zone-A as an input into the EMV. Prior study by Ajibola et al. (2015) highlighted the incapability of the proxy model to capture non-linearity/curvature, there are limits to the duplication of reservoir performance and
recovery mechanisms which introduces the need to return to the application and resolving the use of ED to quantify the risk of sidetrack/recompletion time.

II. NUMERICAL SIMULATION MODEL OF SYNTHETIC OILFIELDS

The model considered for this study is a production well consisting of parent bore is perforated in a zone (layer), and a secondary (sidetrack leg) open to flow at another zone and specific time with another injection well for secondary recovery under waterflood.

Model for Secondary Recovery using Water Flooding

Structure, reservoir rock and fluid properties and others are given in Table 1 and Table 2, while relative permeability curve is presented in Fig. 3. Layer 1 (L1) is termed as Zone-A and Layer 3 (L3), Zone-B. Layer 2 is essentially a shale break with Net-to-Gross of 0. Rock properties for Zone-A are uncertain with respect to porosity, permeability, thickness and initial reservoir pressure.

The synthetic field used for this case follows that of Orodu et al. (2011). Some of the structure and properties of the reservoir simulation model are given in Table 1. While the production well is located at one end and injection well at opposite end of the reservoir block system.

These are further discussed under experimental design setup in the next section. Maximum oil production and water-cut for control are 3000stb/d and 0.85 for production from Zone-A and 20000stb/d and 0.85 for Zone-B. Production well is located at the centre of the reservoir block system and perforated at Zone-A and Zone-B respectively.

.

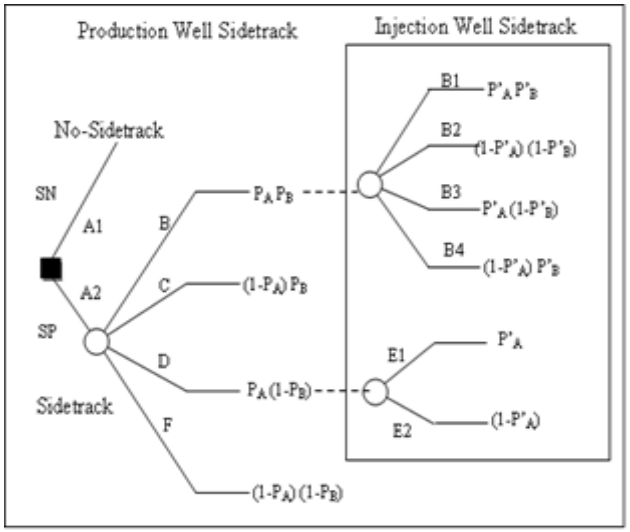

Fig. 1: Decision tree diagram for production well sidetrack/recompletion (primary recovery mechanism) and combined production and injection wells sidetrack/recompletion (secondary recovery mechanism). Orodu & Tang (2011).

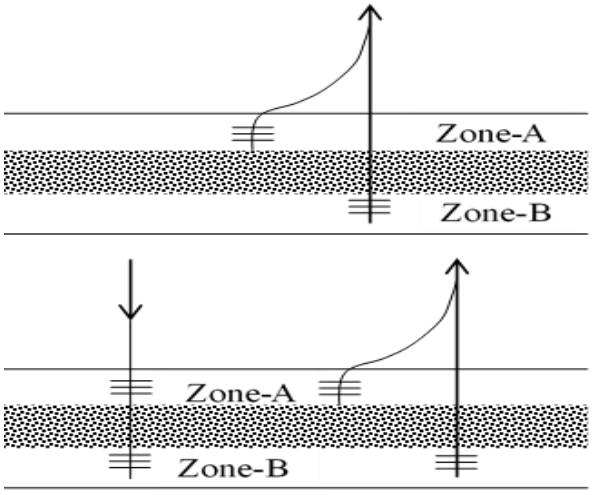

Fig.2: Well(s) configuration (a) primary recovery mechanism (b) secondary recovery mechanism

Table 1: Structure and reservoir rock and fluid properties

Dimension	20*20*5		
Reservoir Tops	6235ft		
Grid Size	Δx=65 ft	Δy=65ft	
	Δz: Layer 1-2 60 - 100 ft	Δz: Layer 3 40ft	Δz: Layer 4-5 80ft
Porosity	Layer 1-2 0.1 - 0.2	Layer 3: 0.12	Layer 4-5: 0.25
Permeability	Layer 1-2: 10 to 20mD	Layer 2: 10mD	Layer 3: 50 mD
Rock Compressibility	1.106E-06 psi^{-1}		
Density (lb_m/ft^3)	Oil: 54.366	Water: 62.43	Gas: 0.0044
Initial Pressure	2320.6 Psi @ 5905ft	3045.8Psi @ 7546ft	

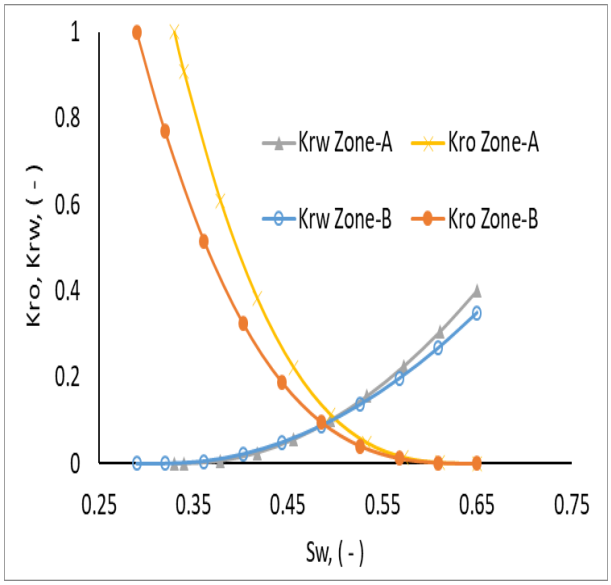

Figure 3 Relative permeability of Zone-A and Zone-B

III. OPTIMAL SIDETRACK TIME FROM OBJECTIVE FUNCTION

This section includes the decision tree set-up to get the Expected Monetary value from generalized NPV model, ED, uncertainty analysis of optimal time by Monte Carlo simulation.

A. Decision Analysis Setup

For the case of simultaneous or sequential sidetrack of production and injection well (Fig. 1), the EMV is:

$$\begin{aligned} EMV_{sidetrack} &= E(Stk) \\ &= P_{B,S}P_{A,S}\left[(B_1+A_2)\acute{P}_{B,S}\acute{P}_{A,S}+(B_2+A_2)\left(1-\acute{P}_{B,S}\right)\left(1-\acute{P}_{A,S}\right)+(B_3+A_2)\left(1-\acute{P}_{B,S}\right)\acute{P}_{A,S}\right. \\ &\quad \left.+(B_4+A_2)\acute{P}_{B,S}\left(1-\acute{P}_{A,S}\right)\right]+P_{B,S}\left(1-P_{A,S}\right)(C+A_2) \\ &\quad +\left(1-P_{B,S}\right)P_{A,S}\left[(E_1+A_2)\acute{P}_{A,S}+(E_2+A_2)\left(1-\acute{P}_{A,S}\right)\right]+\left(1-P_{B,S}\right)\left(1-P_{A,S}\right)(F+A_2) \end{aligned} \quad (1)$$

Where B_1, B_2, B_3, B_4, C, D_1, D_2 and F are the NPV of terminal branches for the scenario. $P_{A,S}$ and $P_{B,S}$ are the POS for the production for Zone-A and Zone-B. and $P'_{A,S}$ and $P'_{B,S}$ for the injection for Zone-A and Zone B.

B. NPV

The economic value of the field is evaluated by the equation:

$$NPV = \sum_{L=1}^{m}\sum_{t=1}^{n}(1+i)^{-t}\left(P_o q_{t,L} - C_{t,L} - I_{t,L}^{F} - I_{t,L}^{V}\right) \quad (2)$$

where *m* is number of layers; *n*, production years; *L*, layer number; *t*, time; *i*, discount rate; P_o, oil price; *q*, production rate; *C*, capital expenditure; *I*, operating expenditure *(F & V)* based on production *F*, fixed and *V*, variable.

Production from both layers are commingled and thus evaluated as a unit. Oil price, discount rate, capital expenditure and fixed operating cost are fixed. While variable operating cost depends on quantity of fluid produced and injected. Oil production from both layers is dependent on simulated rate obtained from a Black Oil simulator based on a synthetic oilfield.

The economic parameters and their values include; discount rate of 12.75%/year or 1.005%/month, oil price of $75/bbl, fixed operating expenditure of 0.25% of capital expenditure and variable operating expenditure is fixed at $5/bbl for production and $2/bbl for water injection. Meanwhile, well drilling and completion for the primary recovery case are $16MM and $5MM for the main-bore and $8MM and $3.75MM for the sidetrack. This aligns with cost in the Niger Delta. For the secondary recovery case, $1MM and $0.5MM (main-bore) and $0.7MM and $0.5MM (sidetrack) in respect of production well. Whilst that of the injection well is $1MM and $0.4MM (main-bore) and $0.7MM and $0.4MM (sidetrack) respectively.

C. Experimental Design and Uncertainty Analysis Parameters

Porosity, permeability, reservoir pressure, thickness and sidetrack time are the uncertain parameters chosen for this study of layer for Zone-A. This is with the assumption that the already producing Zone-B is already appraised and has high quality and quantity of data available due to the status of the well. These uncertain parameters given above are all associated with estimation of reserves, quality of the reservoir, connectivity or pressure depletion state with regards to pressure and they are also usually applied for response surface modelling of reservoir performance as seen in Dejean & Blanc (1999), Prada & Cunha (2008), Esmaiel et al. (2005) and Amorim & Moczydlower (2007), Li et al. (2001), Yeten et al. (2005), Murtha et al. (2009), Narahara et al. (2004),.

The normal technique used involves screening of relevant parameters that affects the study objective, they are the so-called heavy-hitters for detailed analysis using response surface tools. Based on the revelation of a non-linearity issue stated in previous studies the focus to study non-linearity due to sidetrack-time as an independent parameter called for the use of central composite design and varying the point under investigation and also analyzing multiple designs with fixed range of uncertainty of permeability, porosity, pressure and layer-thickness with varying range of time. The main-effects plot is used to differentiate the region of interest and curvature.

Different experimental design runs, response surface and dynamic reservoir models would be created for each branch of the decision tree based on the combination of probabilities of success of Zone-A and Zone-B. The number of experimental runs created is dependent upon the ED or RSM design, number of factors and level.

D. Optimization Function

In order to evaluate and further optimize the objective function, EMV, equations 1 and 2 are used respectively. B_1, B_2, B_3, B_4, C, D_1, D_2 and F are the NPV of terminal branches. NPV is a proxy model which is based on the number of experimental runs and the dynamic reservoir model gives the independent parameters in Eq. (2). However, NPV of terminal branches "C" and "F" are specifically dependent on sidetrack time since no production from Zone-A and the uncertainties considered are only parameters of Zone-A. Hence a regression model is used to fit the response without the need for multiple experimental runs. All proxy model equations are shown in the results section.

E. Monte Carlo Simulation

Uncertain parameters are used to calculate the optimal time computed. Uncertainty analysis is carried out by Monte Carlo simulation with multiple runs based on uniform distribution of each parameter.

IV. RESULTS

The work-flow of secondary recovery by waterflooding are emphasized. This includes analysis of the proxy model by split design, application to optimal time computation based on the multi-objective function and uncertainty analysis of sidetrack time by Monte Carlo simulation.

A. ED and Proxy Model

As in the case for primary recovery with active water drive in the first paper of this series, the same procedure and explanation are applicable with similar trends.

The proxy models of each terminal branch ("B1", "B2", "B3", "B4", "C", "D1", "D2" and "F") are herein presented below having Table 2 showing the bounds of the experimental design.

Table 2: Minimum, mid-point and Maximum points for ED

Factor	Minimum	Base	Maximum
Porosity	0.10	0.15	0.20
Permeability	10 md	15 md	20 md
Layer-thickness	60 ft	80 ft	100 ft
Time	0yrs	5yrs	10yrs

(i) Branch "B1"

Eq. 10 and Fig. 4a is the proxy model and main effect plot for Branch-B1. Time happens to be the major factor controlling NPV, from the plot, the curvature is not severe therefore the model will stand the test of predicting NPV for different inputs of the independent parameters

$$NPV_{B1} = 39.19 + 0.397t + 0.1577h + 67.9\phi + 0.1382k + 0.08583t^2 - 0.01751tk - 8.345t\phi + 0.517h\phi \quad (10)$$

where R-sq, R-sq(adj) and R-sq(pred) are 0.9960, 0.9942 and 0.9903 respectively

(ii) Branch "B2"

The non-linearity laden model of Branch-B2 is presented in Eq (11) and Fig. 4b.

$$NPV_{B2} = -2.739 + 14.0785t + 0.00458h - 0.57\phi + 0.0333k - 0.887422t^2 - 0.001316k^2 - 0.001008th - 0.5813t\phi + 0.0778h\phi + 0.1346\phi k \quad (11)$$

where R-sq, R-sq(adj) and R-sq(pred) are all 1.0.

The following equations (Eq. 12a-c) and figures 4c-d are for the split design scenario to better fit the simulation result of Branch-B2.

$$NPV_{B_2} = \begin{cases} 0 \le t \le 5: NPV_{B2_{0-5}} \\ 5 \le t \le 10: NPV_{B2_{5-10}} \end{cases} \quad (12a)$$

$$NPV_{B2_{0-5}} = -2.831 + 0.00643h + 0.02104k - 1.233\phi + 21.5690t - 0.001127k^2 - 2.37342t^2 + 0.08052h\phi - 0.001440ht + 0.1942k\phi - 0.7276\phi t \quad (12b)$$

where R-sq, R-sq(adj) and R-sq(pred) are all 1.0.

$$NPV_{B2_{5-10}} = 36.891 + 0.00850h + 0.03995k + 1.454\phi + 2.0850t - 0.000815k^2 - 0.087370t^2 + 0.05205h\phi - 0.001033ht + 0.0716k\phi - 0.001906kt - 0.4350\phi t \quad (12c)$$

(iii) Branch "B3"

Eq. (13) and Fig. 4e are similar to that of the curvature laden one of Branch-B2

$$NPV_{B_3} = -11.76 + 14.387t + 0.1486h + 59.9\phi + 0.1521k - 0.80991t^2 - 0.01733th - 7.949t\phi + 0.563h\phi \quad (13)$$

where R-sq, R-sq(adj) and R-sq(pred) are 0.9994, 0.9991 and 0.9984 respectively.

As in the above Branch-B2, the split design equations (Eq. 14a-c) and main effect plots (Fig. 4f-g) are presented below for Branch-B3.

$$NPV_{B_3} = \begin{cases} 0 \le t \le 5: NPV_{B3_{0-5}} \\ 5 \le t \le 10: NPV_{B3_{5-10}} \end{cases} \quad (14a)$$

$$NPV_{B3_{0-5}} = -26.87 + 0.3070h + 1.032k + 72.0\phi + 23.027t - 0.000782h^2 - 0.02325k^2 - 143.2\phi^2 - 2.3216t^2 - 0.00342hk + 0.771h\phi - 0.02214ht + 1.293k\phi - 0.02196kt - 10.197\phi t \quad (14b)$$

where R-sq and R-sq(adj) are 0.9999 and 0.9998 respectively.

$$NPV_{B3_{5-10}} = 33.13 + 0.1355h + 0.1094k + 55.6\phi + 1.486t + 0.422h\phi - 0.01253ht - 5.702\phi t \quad (14c)$$

where R-sq, R-sq (adj) and R-sq (pred) are 0.9938, 0.9912 and 0.9892 respectively

(iv) Branch "B4"

Proxy model (Eq. 15) is suitable for application as Fig. 4h shows the main effect plot been relatively linear as a predictive tool.

$$NPV_{B4} = 46.102 + 0.2520t + 0.00706h + 4.04\varphi + 0.008737t^2 - 0.001179th - 0.6923t\phi + 0.0734h\phi \quad (15)$$

where R-sq, R-sq (adj) and R-sq (pred) are 0.9979, 0.9972 and 0.9931 respectively.

(v) Branch "C"

Regression analysis model for Branch-C is presented in equation Eq. (16). The reason is to capture the NPV from the simulation as production ends at 7.915 years resulting in change of trend line.

$$NPV_C = \begin{cases} 0 \le t \le 5: NPV_{C_{0-7.915}} = 47.464 + 0.1699t - 0.0069t^2 \\ 5 \le t \le 10: NPV_{C_{7.916-10}} = 47.382 + 0.049t \end{cases} \quad (16)$$

(vi) Branch "D1"

$$NPV_{D1} = -18.02 + 15.288t + 0.1477h + 59.7\phi + 0.616k - 0.85138t^2 - 0.01239k^2 - 0.01720th - 7.924t\phi - 0.01829tk + 0.563h\phi \quad (17)$$

where R-sq, R-sq(adj) and R-sq(pred) are 0.9996, 0.9994 and 0.9987 respectively.

$$NPV_{E1} = \begin{cases} 0 \le t \le 5: NPV_{E2_{0-5}} \\ 5 \le t \le 10: NPV_{E2_{5-10}} \end{cases} \quad (18)$$

$$NPV_{E1_{0-5}} = -18.34 + 0.2204h + 0.1980k + 90.6\phi + 23.84t - 2.4712t^2 - 0.0219ht - 10.15\phi t \quad (19)$$

where R-sq, R-sq(adj) and R-sq(pred) are 0.9974, 0.9964 and 0.9933.

$$NPV_{E1_{5-10}} = 27.94 + 0.1063h + 0.436k + 45.12\phi + 2.151t - 0.00661k^2 - 0.0288t^2 - 0.001653hk + 0.4216h\phi - 0.01253ht + 0.697k\phi - 0.01343kt - 5.702\phi t \quad (20)$$

where R-sq, R-sq(adj) and R-sq(pred) are 0.9978, 0.9956 and 0.9922 respectively.

(vii) Branch "D2"

As in Branch-D1 above, the same trend is observed as seen in Fig.4l and Fig. 4m-n and the models presented in Eq. (21) and 22 (a-b).

$$NPV_{E2} = -5.854 + 14.8162t + 0.00735h + 1.91\phi + 0.0470k - 0.932252t^2 - 0.000854k^2 - 0.001229th - 0.5586t\phi - 0.001223tk + 0.0699h\phi \quad (21)$$

where R-sq, R-sq (adj) and R-sq (pred) are all 1.0

$$NPV_{E2} = \begin{cases} 0 \le t \le 5: NPV_{E2_{0-5}} \\ 5 \le t \le 10: NPV_{E2_{5-10}} \end{cases} \quad (22a)$$

$$NPV_{E2_{0-5}} = -5.361 + 0.00423h + 0.0277k - 1.65\phi + 22.0566t - 0.000913k^2 - 2.37879t^2 \quad (22b)$$

where R-sq, R-sq(adj) and R-sq(pred) are all 1.0.

$$NPV_{E2_{5-10}} = 32.83 + 0.0903h + 2.419t - 0.0702t^2 - 0.00990ht \quad (23)$$

where R-sq, R-sq(adj) and R-sq(pred) are 0.932, 0.9184 and 0.8101 respectively.

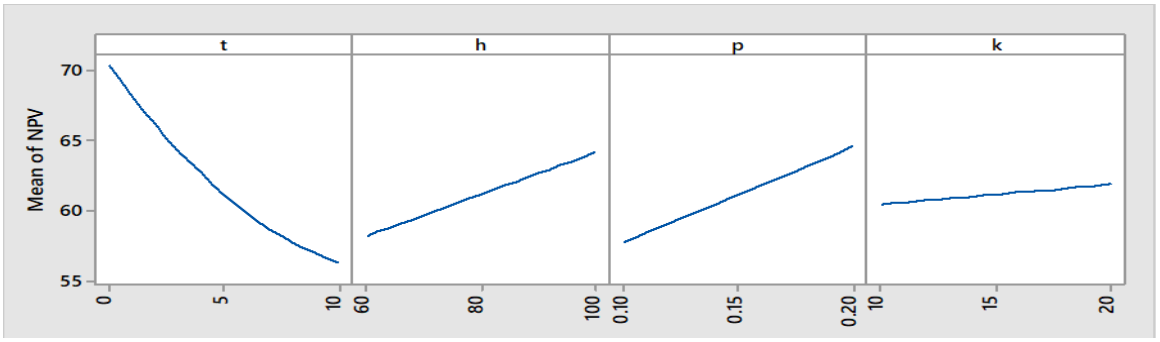

Fig. 4a: Main effect plot for Branch-B1

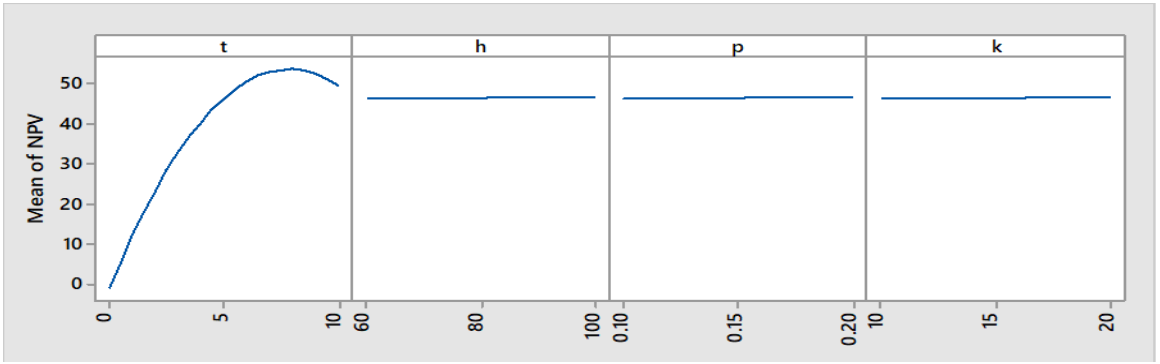

Fig. 4b: Main effect plot for Branch-B2

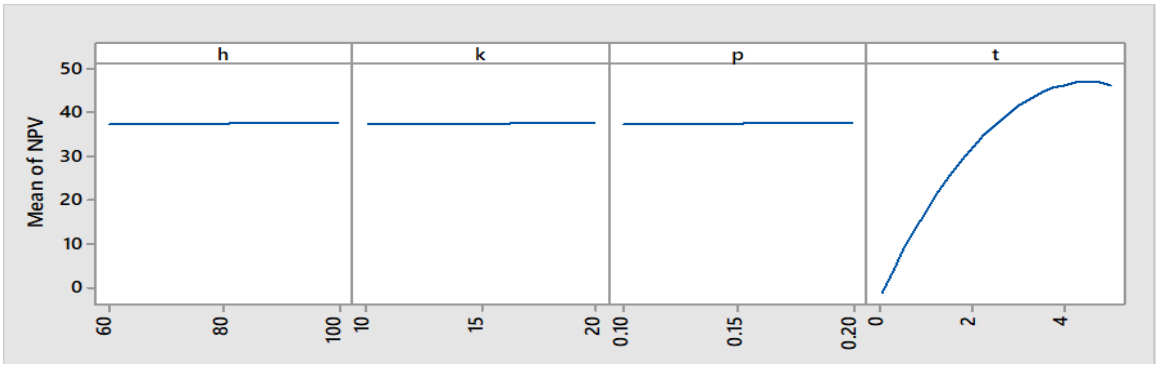

Fig. 4c: Main effect plot for split-design 0 to 5 years for Branch-B2

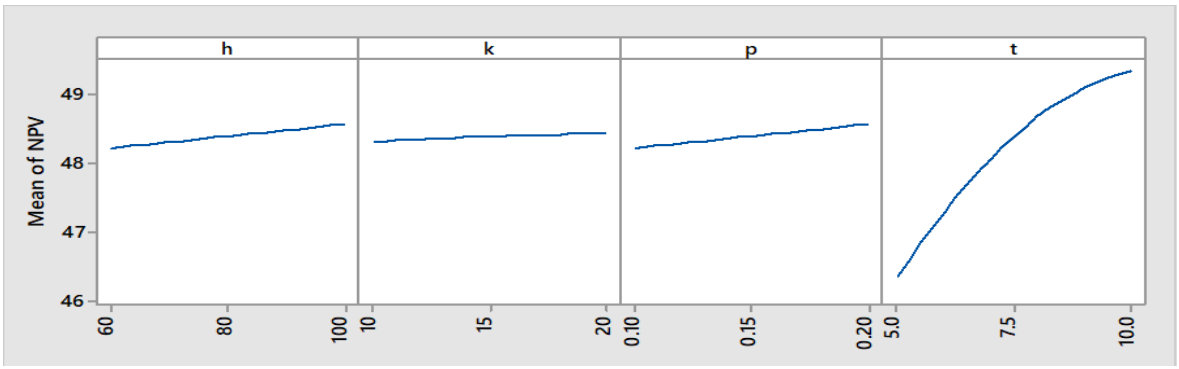

Fig. 4d: Main effect plot for split-design 5 to 10 years for Branch-B2

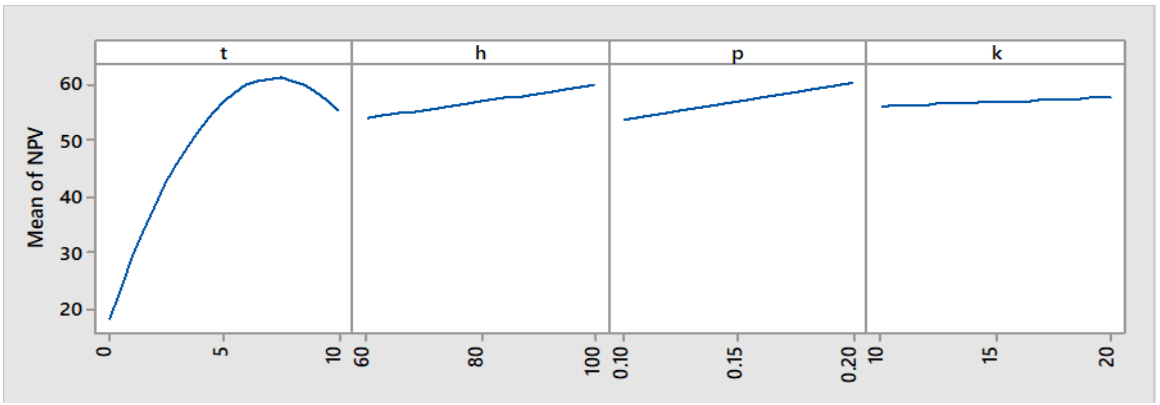

Fig. 4e: Main effect plot for Branch-B3

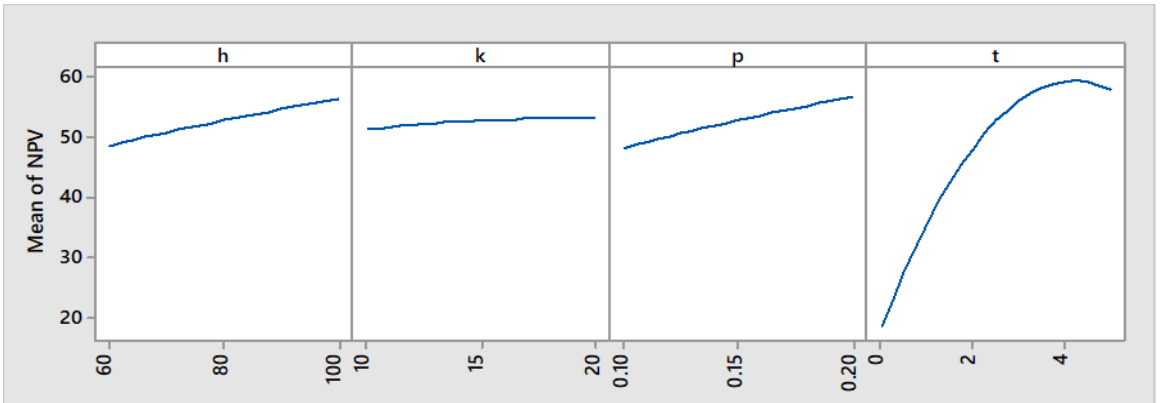

Fig. 4f: Main effect plot for split-design 0 to 5 years for Branch-B3

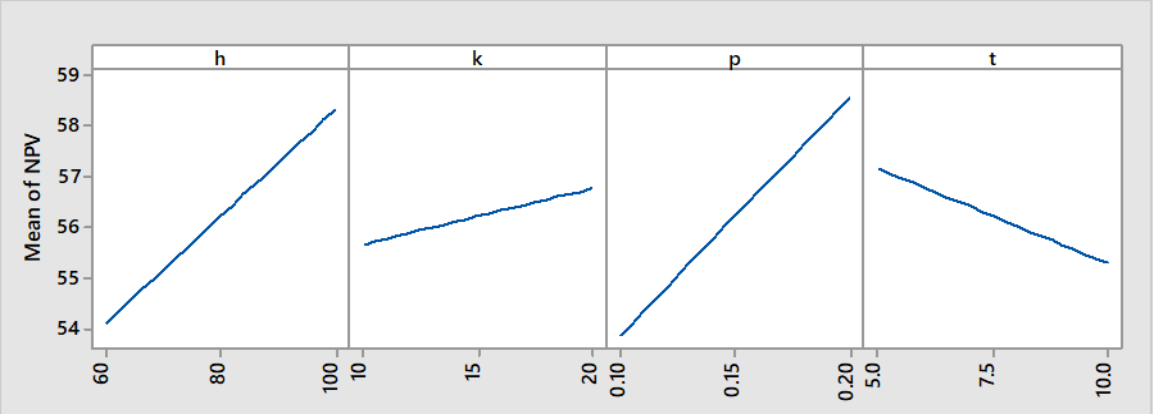

Fig. 4g: Main effect plot for split-design 5 to 10 years for Branch-B3

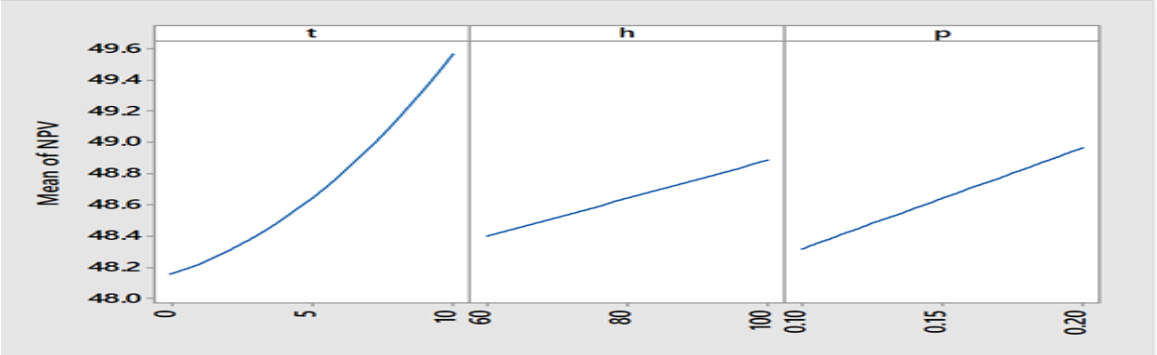

Fig. 4h: Main effect plot for Branch-B4

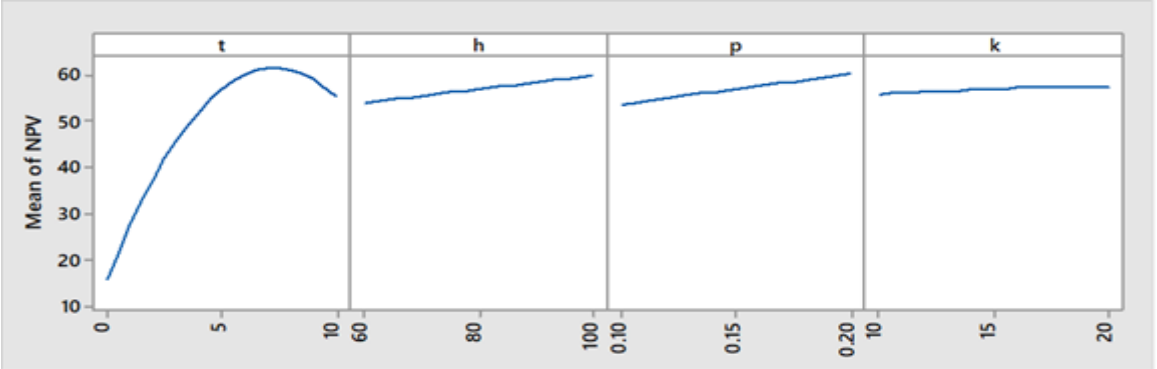

Fig. 4i: Main effect plot for Branch-D1

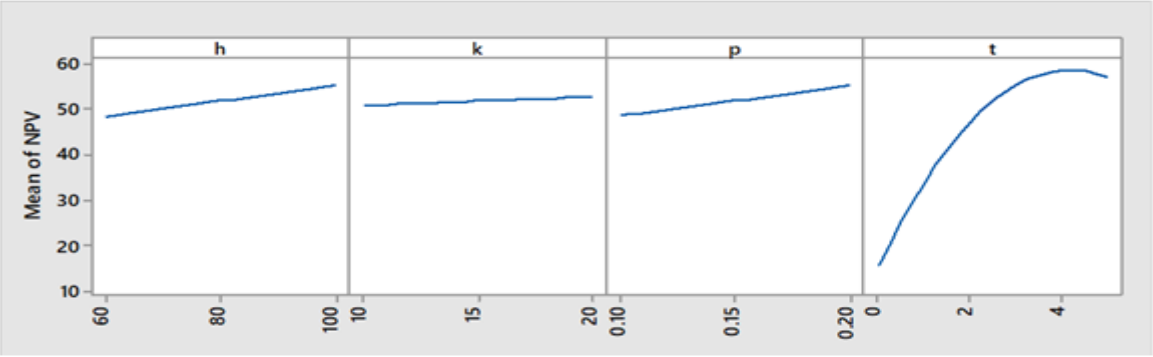

Fig. 4j: Main effect plot for split-design 5 to 10 years for Branch-D1

II. Secondary Recovery Mechanism

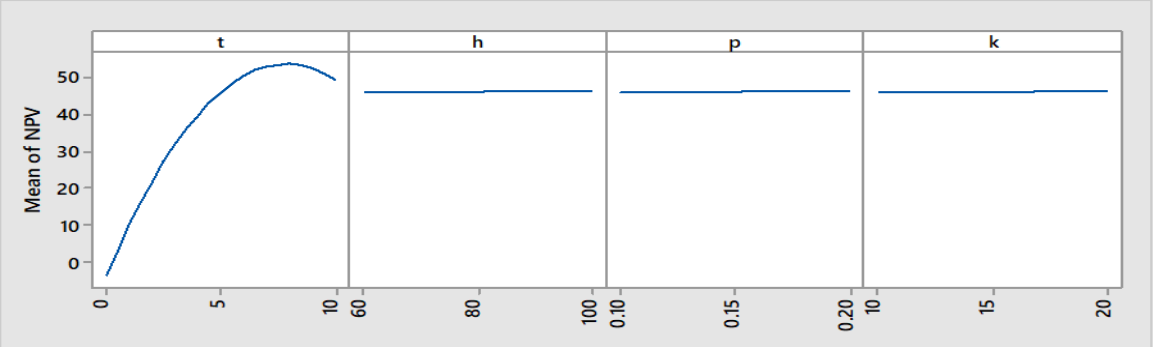

Fig. 4k: Main effect plot of Branch-D2

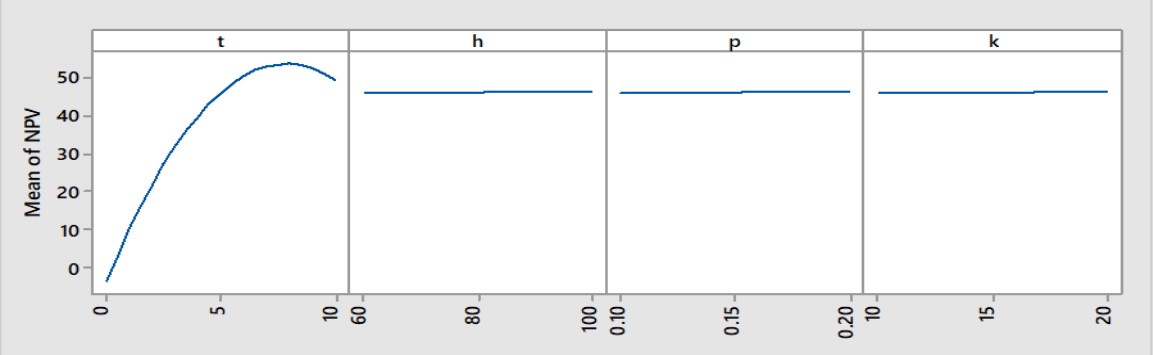

Fig. 4l: Main effect plot of Branch-D2

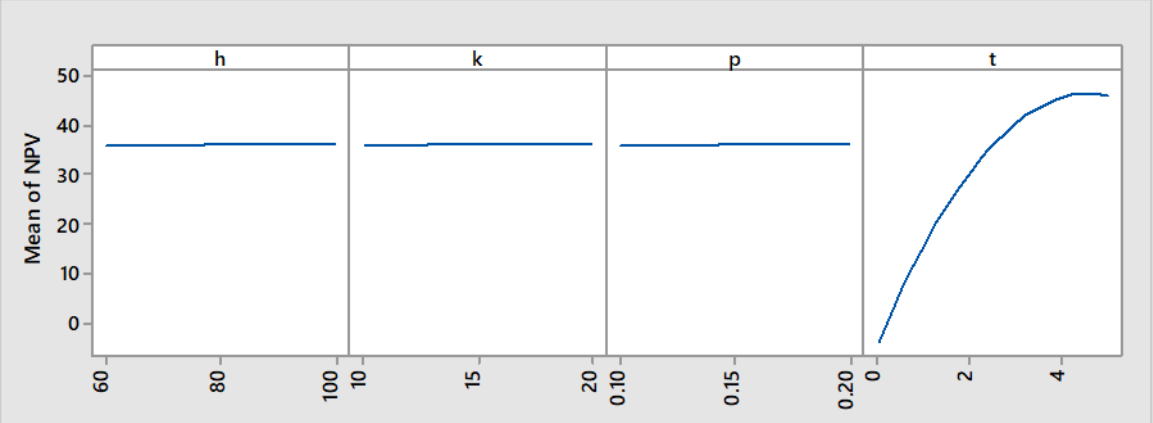

Fig. 4m: Main effect plot for split-design 0 to 5 years for Branch-D2

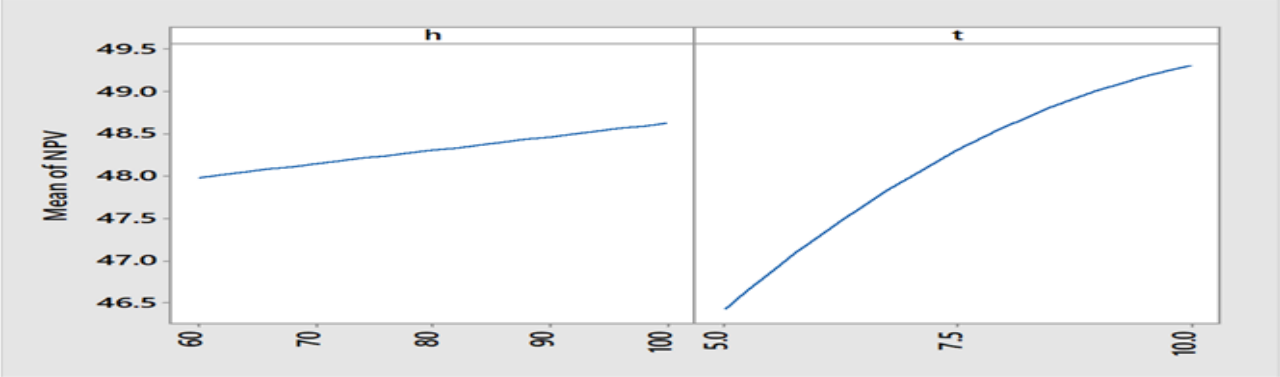

Fig. 4n: Main effect plot for split-design 5 to 10 years for Branch-D2

B. Optimal Sidetrack/Recompletion Time

Tests were conducted on the applicability of the proxy and regression models based on the factors used. Values of 70 ft., 18 md and 0.14 for layer-thickness, permeability and porosity respectively and at time intervals of 2 years from 0 to 10 years. Fig. 5a-b shows the reasonable match of proxy models to the simulation results for all the terminal branches. Split-design models were applied in all cases where applicable as in the previous case of primary recovery. In comparing Fig. 5a-b for proxy models to that of Fig. 6 for analytical models (Orodu et al., 2011), the former's performance is acceptable and better off for some terminal branches like "B4" and "D2". The lump in the curve for branches "B2", "B3", "D1" and "D2" can further be resolved by increasing the intervals of the split design from 2 to 3 to further reduce the effect of curvature.

Fig. 7 shows the match of EMV at POS of $P_A = P'_A = 0.5$ and $P_B = P'_B = 0.9$. Optimal sidetrack-time is approximately 4 years with a correlation coefficient of 0.9999. A more detailed evaluation of the performance of the proxy model is as depicted in Fig. 8a-d. Match in Fig. 8c – d cannot be said to be poor as the difference in EMV from 6 years to 10 years is not significant. On overall, the proxy model performance is acceptable for optimisation study.

Monte Carlo simulation was conducted on the proxy model of EMV to study the impact of uncertainty of the factors on sidetrack-time with 3000 runs. Number of runs was investigated for stability after initially trying 10,000 runs and analysing with mean. 3000 runs were adjudged suitable for further studies. Uncertainty analysis of the optimal sidetrack-time shows a tilt of bulk results towards low time (<5 years) and a spike under favourable POS, this is as expected (see Fig. 9a-c). For slightly unfavourable results, there tends to be a spread of sidetrack-time, multimodal distribution and fairly increasing clusters towards the 10^{th} year (Fig. 9b). However, the trend in Fig. 9b is unexpected and cannot be said to fall under unfavourable POS conditions as likely favourable POS should translate to clustering of sidetrack-time at early years of the field development. The trend for EMV at optimal sidetrack-time is similar for all the POS combinations of Fig. 9 as seen in Fig. 10 for P_A and P_B=0.5; P'_A and P'_B=0.5 according to Fig. 9a. Distribution of EMV is either multimodal (multiple normal distribution) in nature or simply a log-normal distribution that is skewed to the right.

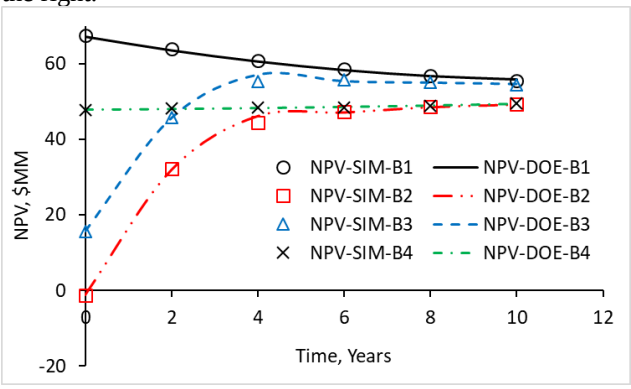

Fig. 5a: NPV plot for comparison of simulation results and proxy and regression models for terminal branches "B1", "B2", "B3" and "B4".

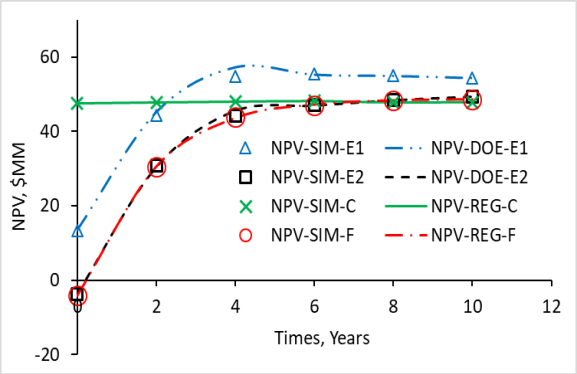

Fig. 5b: NPV plot for comparison of simulation results and proxy and regression models for terminal branches "C" "D1", "D2" and "F4"

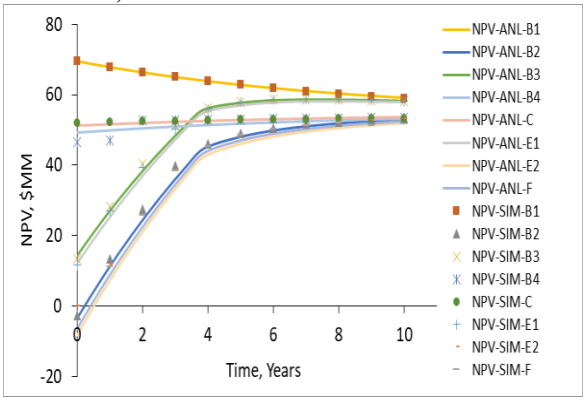

Fig. 6: NPV of terminal branches "B1", "B2", "B3", "B4", "C" "D1", "D2" and "F4" for simulation and analytical model. Adapted from (Orodu et al., 2011)

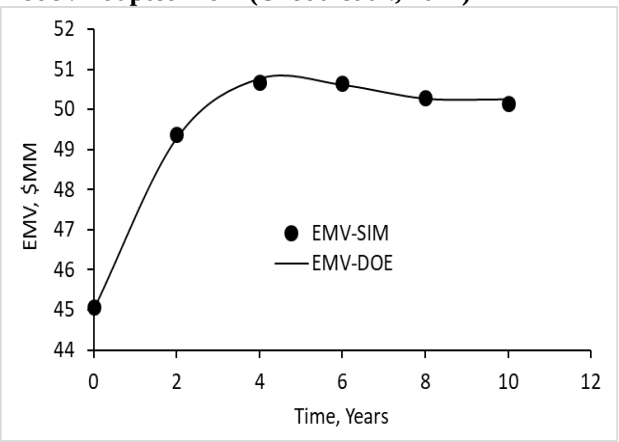

Fig. 7: EMV plot for comparison of simulation and design of experiment for POS ($P_A = P'_A = 0.5$ and $P_B = P'_B = 0.9$).

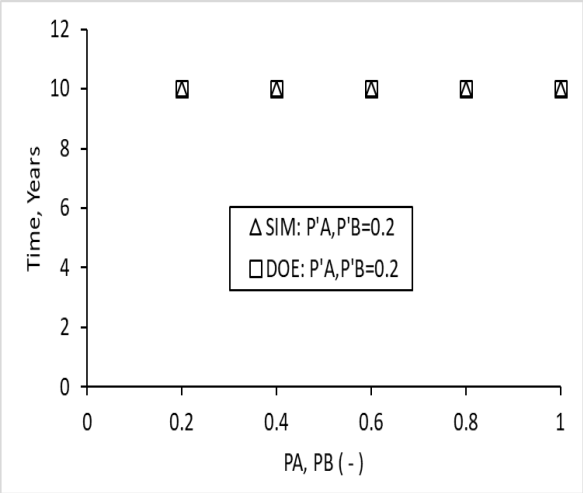

Fig. 8a: Sidetrack time from simulation and experimental design for P'_A and P'_B = 0.2

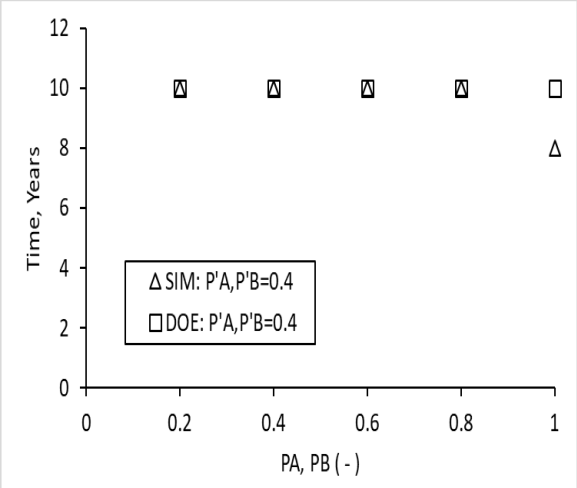

Fig. 8b: Sidetrack time from simulation and experimental design for P'_A and P'_B = 0.4

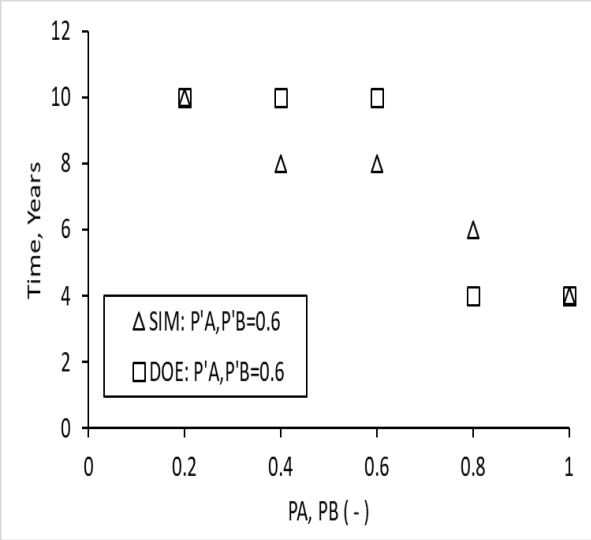

Fig. 8c: Sidetrack time from simulation and experimental design for P'_A and P'_B = 0.6

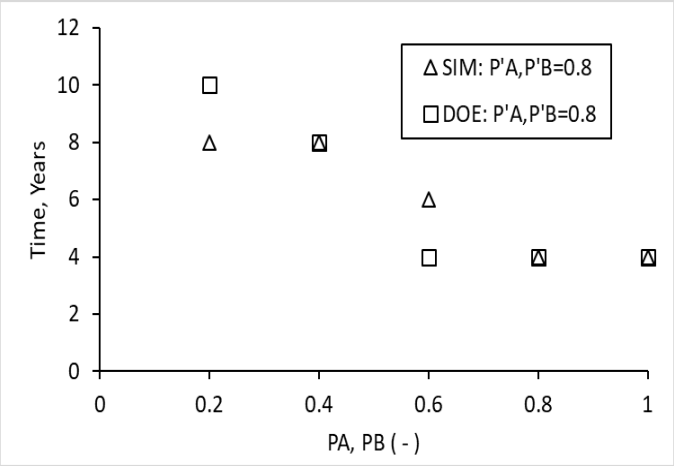

Fig. 8d: Sidetrack time from simulation and experimental design for P'_A and P'_B = 0.8

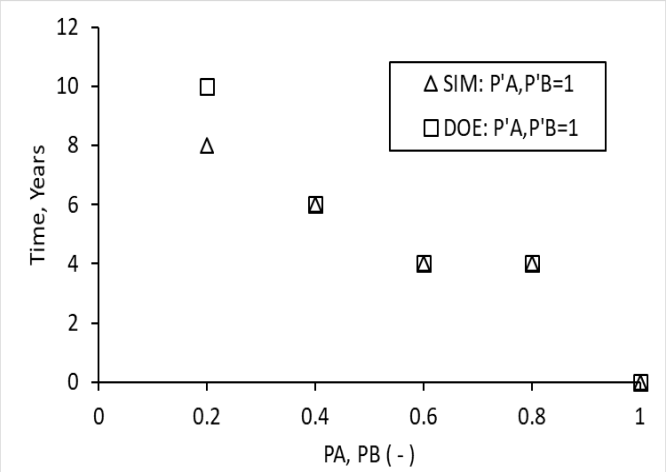

Fig. 8e: Sidetrack time from simulation and experimental design for P'_A and P'_B = 1.0

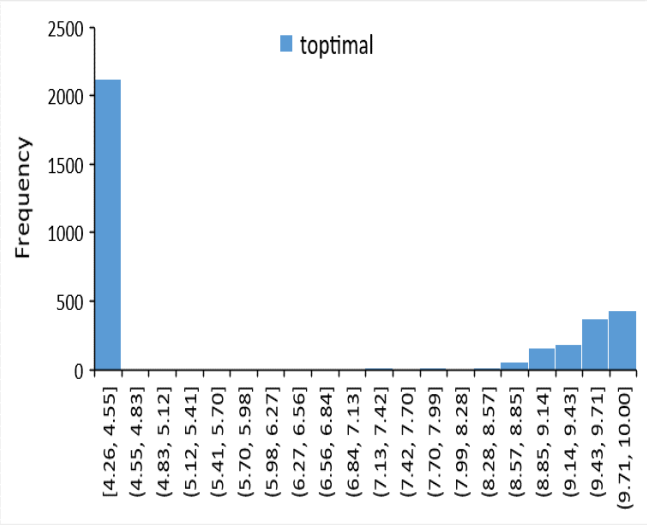

Fig. 9a: Optimal sidetrack time distribution at P_A and P_B = 0.5; P'_A and P'_B = 0.5

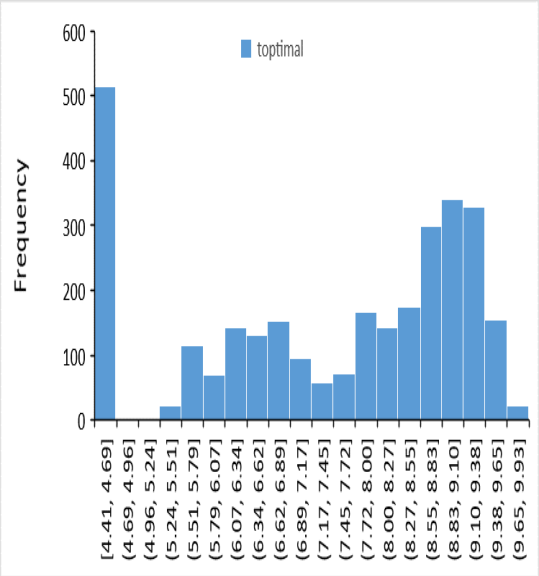

Fig. 9b: Optimal sidetrack time distribution at P_A and P_B=0.5; P'_A and P'_B=0.7

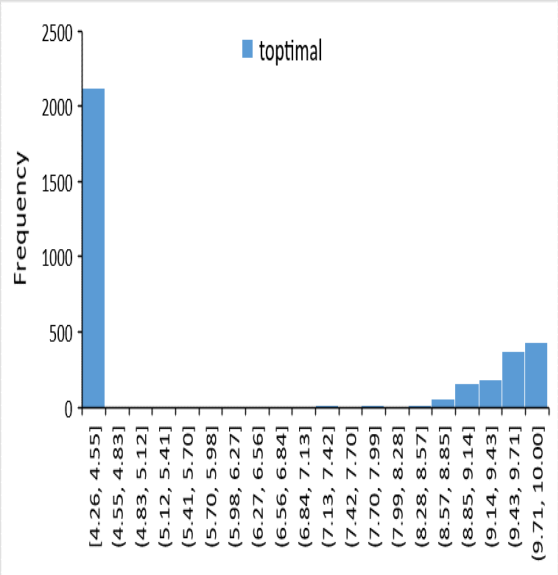

Fig. 9c: Optimal sidetrack time distribution at P_A and P_B=0.7; P'_A and P'_B=0.5

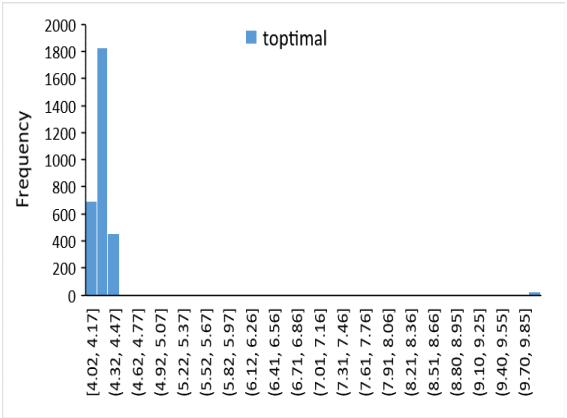

Fig. 9d: Optimal sidetrack time distribution at P_A and P_B=0.7; P'_A and P'_B=0.7

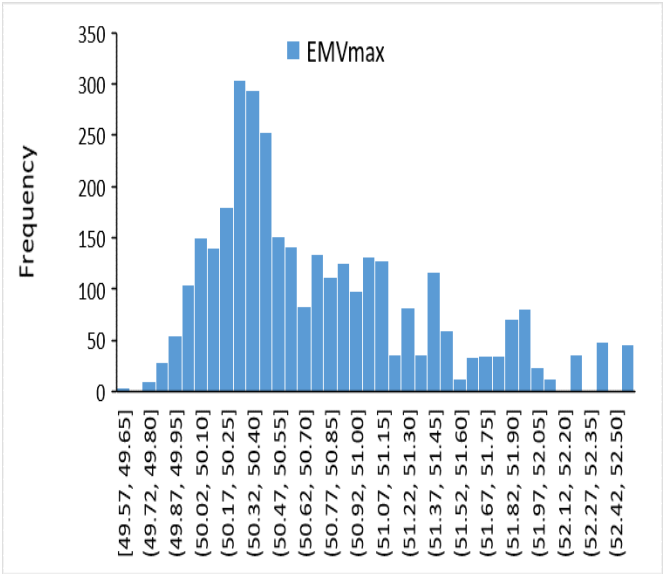

Fig. 10: Maximum EMV for run at P_A and P_B=0.5; P'_A and P'_B=0.5

C. Split Design Performance

In this study, dynamic proxy models were used and time was included to evaluate EMV while considering uncertainties. Multi-objective function has been aptly used through implementing split design to solve for non-linearity introduced by sidetrack time for some of the terminal branches of the decision tree as evident in the main effect plots. In order to increase precision more time intervals can be applied but this introduces more runs therefore more time which is costly.

The effect of time on proxy models had been noted by Dejean & Blanc (1999) in the construction of models for cumulative oil produced at specific and incremental time intervals. It was noted that models for earlier time periods were insignificant while those at later stages was significant. Reason(s) for the trend observed was neither investigated nor explained. However, the case can be explained by the changed in the mechanism(s) controlling flow at the micro-scale of the reservoir rock.

An approach by Panjalizadeh et al. (2014) may serve as a means of navigating away from the added time of optimization for the method developed in this study. A combination of 3-level full factorial design and Inscribed Central Composite design was applied to resolve the curvature that arose from a time dependent model on cumulative oil production. The point to note is that application of ED should be fit-for-purpose, dependent on severity of non-linearity. For the current study, the severity is akin to that of a scaling the hurdle of a dog-leg as in drilling operations and that of the above authors was less severe. Outright modelling of NPV is further laced with the influence of the time-value of money in respect to that of cumulative oil production. Be it as it may, combination of either Box-Behnken and Central Composite designs or Full Factorial and Central Composite design is gaining popularity in application as seen in Kang et al. (2016).

In effectively having a time-based dynamic proxy-model, non-conformity of derivatives of models in solving rate-based analytical equations will be rendered possible (Lawal, 2009). Thereby, enhancing the use of proxy models.

Conclusion

The optimal time for sidetrack has been optimized while considering uncertainties and the high non-linearity was solved using split-plot design of various time-intervals, increasing experimental runs by a multiple of two which lead to multiple proxy models over a decision scenario and multi-objective optimization scheme for the expected monetary value (EMV) model.

Though the point of split into time-intervals was qualitative, albeit, based on main effect plots of independent input variables gave quite significant results as observed on testing and validation. It resulted in increase in number of experimental runs as already elaborated in literature to solve non-linearity. Attempts at combining the runs over the time-intervals gave poorly defined proxy models.

Accuracy achieved by the developed method actually replicates past performance based on use of analytical and empirical models as predictive tools for cumulative produced oil. This enabled the use of the equations as input for setting up the EMV objective function. The accuracy can be substantially improved by increasing the number of intervals; however, it makes for increase in runs for experimental design and run-time for optimization. The slight disparity noticed was for negligible and reduced difference in EMV at late time of the field production life.

Use of numerical simulation for this study clearly underscores its importance as a tool for uncertainty analysis with the capability to depict various recovery scenarios over analytical and empirical models.

The Probability of success (POS) parameter for optimizing sidetrack time has a major effect on it, risk and geological uncertainties are contained in this term. As expected, positive and high POS means early sidetrack time and otherwise it signifies carrying out the sidetrack operation at latter times.

REFERENCES

1. Ajibola, J.T., Orodu, K.B. & Orodu, O.D. (2015) Sidetrack/Recompletion Time Evaluation by Proxy Model, International Journal of Petroleum Technology, 2:18-28
2. Amorim, T. & Moczydlower, B. (2007) Validating the use of experimental design techniques in exploratory evaluations, SPE Paper 107441 presented at the SPE Latin American & Caribbean Petroleum Engineering Conference, 15-18 April, Buenos Aires, Argentina
3. Artun, E., Ertekin, T., Watson, R. & Al-Wadhahi, M. (2011) Development of universal proxy models for screening and optimization of cyclic pressure pulsing in naturally fractured reservoirs, Journal of Natural Gas Science and Engineering, 3(6): 667-686
4. Dejean, J.P. & Blanc, G. (1999) Managing Uncertainties on Production Predictions Using Integrated Statistical Methods, SPE Paper 56696 presented at the SPE Annual Technical Conference and Exhibition, 3-6 October, Houston, Texas
5. Egeland, T., Holden, L. & Larsen, E.A. (1992) Designing Better Decisions, SPE Paper 24185 presented at European Petroleum Computer Conference, 24-18 May, Stavanger, Norway
6. Esmaiel, T.E., Bolandtaba, S.F. & van Kruijsdijk, C. (2005) Reservoir Screening and Sensitivity Analysis of Waterflooding with Smart Wells through the Application of Experimental Design, SPE Paper 93568 presented at SPE Middle East Oil and Gas Show and Conference, 12-15 March, Kingdom of Bahrain
7. Garb, F.A. (1988) Assessing risk and uncertainty in evaluating hydrocarbon-producing properties, Journal of Petroleum Technology 40(6):765-778.
8. Ghasemzadeh. S. & Charkhi, A.H. (2016) Optimization of integrated production system using advanced proxy based models: Anew approach, Journal of Natural Gas Science and Engineering, 35: 89-96.
9. Jourdan, A. & Zabalza-Mezghani, I. (2004) Response surface designs for scenario management and uncertainty quantification in reservoir production, Mathematical Geology, 36(8): 965-985
10. Kang, C.A., Brandt, A.R. & Durlofsky, L.J. (2016) A new carbon capture proxy mode for optimizing the design and time-varying operation of a coal-natural gas power station, International Journal of Greenhouse Gas Control, 48:234-252.
11. Lawal, K.A. (2009) Modelling Subsurface Uncertainties with Experimental Design: Some Arguments of Non-Conformists, SPE Paper 128350 presented at the Nigeria Annual International Conference and Exhibition, 3-5 August, Abuja, Nigeria
12. Lerche, I. & Mudford, B., 2001. Risk evaluation for recompletion and sidetrack developments in oil fields. SPE Paper 71418, SPE Annual Technical Conference and Exhibition, New Orleans, 30 September–2 October.
13. Lerche, I. & Noeth, S., 2004. Economics of Petroleum Production — A Compendium Volume 1: Profit and Risk. Multi-Science Publishing Co., Essex
14. Li, H., Sarma, P. & Zhang, D. (2011) A Comparative Study of the Probabilistic-Collocation and Experimental-Design Methods for Petroleum-Reservoir Uncertainty Quantification, SPE Journal 16(2): 429-439.
15. Murtha, J.A., Osorio, R., Perez, H., Kramer, D.L., Skinner, R.J. & Williams, C.A. (2009) Experimental Design: Three Contrasting Projects, SPE Paper 121878 presented at the Latin American and Caribbean Petroleum Engineering Conference, 31 May-3 June, Cartagena de Indias, Colombia
16. Naderi, M. & Khamehchi, E. (2016) Nonlinear risk optimization approach to water drive gas reservoir production optimization using DOE and artificial intelligence, Journal Natural Gas Science and Engineering, 31: 575–584.
17. Narahara, G.M, Spokes, J.J., Brennan, D.D., Maxwell, G. & Bast, M. (2004) Incorporating Uncertainties in Well-Count Optimization With Experimental Design for the Deepwater Agbami Field, SPE Paper 91012 presented at the SPE Annual Technical Conference and Exhibition, 26-29 September, Houston, Texas
18. Odeh, A.S. (1981) Comparison of Solutions to a Three-Dimensional Black-Oil Reservoir Simulation Problem, Journal of Petroleum Technology 33(1): 13-25.
19. Orodu, O.D. & Tang Z.(2011) Risk Evaluation Production-Injection Recompletion and Sidetrack, Energy Exploration and Exploitation; 29 (3): 235-250.
20. Orodu, O. D., Tang, Z. and Anawe, P. A. L. (2011) "Sidetrack and Recompletion Risk Evaluation - Waterflooded Reservoir", Journal of Petroleum Science and Engineering, 78(3-4):705-718.
21. Osterloh, T.W. & Menard, W.P. (2007) New Method Combines Simulation and Novel Spreadsheet Tools to Enable Direct Optimization of Expansion Decisions in a Giant Heavy-Oil Field, SPE Reservoir Evaluation & Engineering 10(1): 35-42.
22. Panjalizadeh, H., Alizadeh, N. & Mashhadi, H. (2014) A workflow for risk analysis and optimization of steam flooding scenario using static and dynamic proxy models, Journal of Petroleum Science and Engineering, 121: 78-86.
23. Prada, V.J.W. & Cunha, L.B. (2008) Prediction of SAGD Performance Using Response Surface Correlations Developed by Experimental Design Techniques, Journal of Canadian Petroleum Technology, 47(9):58-64
24. Shook, M.G., Walker, D.L., Kackson, A.C., Ruby, N.H. & Poulsen, A. (2014) Optimizing Field Development of Greenfield Polymer Floods Using Experimental Design, SPE Paper 170007 presented at the SPE Heavy Oil Conference-Canada, 10-12 June, Calgary, Alberta, Canada
25. Yeten, B., Castellini, A., Guvaguler, B. & Chen, W.H. (2005) A Comparison Study on Experimental Design and Response Surface Methodologies, SPE Paper 93347 presented at the SPE Reservoir Simulation Symposium, 31 January-2 Feburary, The Woodlands, Texas

AUTHORS PROFILE

Abisoye M. Mumuni,
BSc. Petroleum Engineering (Covenant University); MSc. Petroleum Engineering, (Dalhousie University) &
PhD Student, CEFOR-ACE, World-Bank University of Port-Harcourt, Nigeria.

Oyinkepreye Orodu,
Professor, Head of Department, Petroleum Engineering, Covenant University, Nigeria. BSc. Chemical Engineering; MSc. Oil & Gas Engineering &
Doctorate in Petroleum Engineering

Sunday Ikiensikimama,
Associate Professor, Department of Petroleum & Gas Engineering,
University of Port Harcourt, Nigeria.